Geomicrobiology Journal

ISSN: (Print) (Online) Journal homepage: https://www.tandfonline.com/loi/ugmb20

Characterization of Bacterial Exudates Through Potentiometric Titrations

Leah C. Sullivan, Qiang Yu, Joshua D. Shrout & Jeremy B. Fein

To cite this article: Leah C. Sullivan, Qiang Yu, Joshua D. Shrout & Jeremy B. Fein (2024) Characterization of Bacterial Exudates Through Potentiometric Titrations, Geomicrobiology Journal, 41:2, 172-182, DOI: 10.1080/01490451.2023.2300256

To link to this article: https://doi.org/10.1080/01490451.2023.2300256

Published online: 31 Jan 2024.

GEOMICROBIOLOGY JOURNAL
2024, VOL. 41, NO. 2, 172–182
https://doi.org/10.1080/01490451.2023.2300256

Characterization of Bacterial Exudates Through Potentiometric Titrations

Leah C. Sullivan[a], Qiang Yu[a], Joshua D. Shrout[a,b], and Jeremy B. Fein[a]

[a]Department of Civil and Environmental Engineering and Earth Sciences, University of Notre Dame, Notre Dame, IN, USA; [b]Department of Biological Sciences, University of Notre Dame, Notre Dame, IN, USA

ABSTRACT

Bacterial exudates are organic molecules released by bacteria that have proton- and metal-binding capacities, as well as the ability to facilitate redox reactions. However, the binding sites responsible for these functions are poorly characterized. In this work we examine the concentrations and types of proton active sites through potentiometric titrations of exudate solutions produced from several bacterial species. Additionally, we report the first measurement of sulfhydryl site concentrations of bacterial exudates. Finally, we examine the processes by which these exudates are produced in order to constrain the relative importance of active and passive production of the exudate molecules. Our results demonstrate that, while overall proton-binding behavior is primarily dependent on the amount of organic material produced, the concentration of sulfhydryl sites present on the exudate molecules is species-dependent and is not related to the amount of exudate produced. This result indicates that bulk proton-binding characteristics and total proton-active site concentrations on exudate molecules are relatively constant between species, but that the species of bacteria does impact the functionality of the exudates produced, particularly with respect to binding of chalcophile elements and redox reactions involving those elements.

ARTICLE HISTORY
Received 28 April 2023
Accepted 19 December 2023

KEYWORDS
Bacterial exudates;
sulfhydryl sites;
potentiometric titrations

Introduction

In contrast to extracellular polysaccharides (EPS), which are insoluble and physically bound to bacterial cells, bacterial exudates are soluble organic molecules that are released by bacteria from active production and from cell lysis. Both proteomic and metabolomic approaches have been used to investigate the composition of bacterial products within soils (e.g., Djemiel et al. 2022; Jones et al. 2014; Kawasaki and Benner 2006; Keiblinger et al. 2016; Rochfort et al. 2015; Swenson et al. 2015). Peptidoglycan components, amine sugars, amino acids, carboxylic acids, sugar alcohols, and sterols are all metabolites known to be released by bacteria into the extracellular matrix (Jones et al. 2014; Kawasaki and Benner 2006; Rochfort et al. 2015; Swenson et al. 2015), however very few studies have focused exclusively on the soluble exudate fraction. Although bacterial exudates, like EPS molecules, have the capacity to bind protons and metals and to facilitate redox reactions (Kenney et al. 2012; Ohnuki et al. 2007; Seders and Fein 2011; Sullivan et al. 2022), the important exudate binding site types and their properties remain poorly characterized. FTIR spectroscopy of bacterial exudates indicates that exudate molecules are comprised primarily of polysaccharides and proteins (Seders and Fein 2011). Bacterial exudates contain organic acids with proton-active binding sites (Seders and Fein 2011), but total proton-active binding site concentrations and associated acidity constant (Ka) values have been measured for exudate molecules from only two bacterial species (Seders and Fein 2011). These values are similar between the two species studied, however exudates from a wider range of bacterial species must be studied in order to draw general conclusions about their similarities or lack thereof.

Soluble bacterial exudate molecules are capable of reducing aqueous Au(III) and Se(IV) in the absence of bacterial cells (Kenney et al. 2012; Sullivan et al. 2022). This reduction capacity, in conjunction with the observation that treatment of the bacterial exudate molecules with a sulfhydryl blocking treatment stops at least Se(IV) reduction (Sullivan et al. 2022), strongly suggests that sulfhydryl binding sites are present to some extent on these molecules and may play an important role in the environmental fate of redox-sensitive chalcophile elements. Sulfhydryl sites are present as the active site on a wide range of proteins, commonly serving as electron donors in protein-mediated redox reactions (Fomenko et al. 2008; Giles et al. 2003; Poole 2015). Although sulfhydryl site concentrations have been measured for bacterial surfaces (Joe-Wong et al. 2012; Yu et al. 2014, 2018), the concentration of sulfhydryl sites on bacterial exudate molecules has not been measured, and hence the relative importance of exudate molecules to bacterial surface molecules in sulfhydryl-mediated processes cannot be determined.

One of the objectives of this study was to use potentiometric titrations of bacterial exudate solutions to determine the number of types of proton-active binding sites on the

CONTACT Leah C. Sullivan lsulli10@nd.edu Department of Civil and Environmental Engineering and Earth Sciences, University of Notre Dame, Notre Dame, IN 46556, USA.

exudate molecules along with their site concentrations and associated Ka values, comparing results between exudate solutions from two Gram-positive and two Gram-negative bacterial species. We test whether individual and total site concentrations, normalized to total dissolved organic carbon, are similar between the exudates from different bacterial species. In addition, we used a liquid chromatograph-mass spectrometry (LC-MS) approach (Yu and Fein 2024) in conjunction with a sulfhydryl-specific blocking molecule to determine the concentration of sulfhydryl sites within exudate solutions from the four bacterial species studied. Lastly, because some fraction of the exudates is likely actively produced and secreted by the cells, and another portion of the exudates is produced as byproducts of cell lysis and breakdown, we constrained the relative contribution of each exudate source by measuring the progression of cell lysis over the course of exudate production using LIVE/DEAD staining and confocal microscopy. Our experimental results expand our knowledge of total site concentrations on exudate molecules and represent the first measurements of exudate sulfhydryl site concentrations specifically. These measurements enable quantitative comparisons of the importance of bacterial cell wall binding sites and binding sites on exudate molecules, thereby furthering our understanding of potential influences of each type of ligand on the environmental behavior of metals.

Methods

Exudate production

This study involved exudate solutions from four different bacterial species, each prepared following procedures described by Sullivan et al. (2022). Two Gram-positive bacterial species (*Bacillus subtilis* and *Bacillus licheniformis*) and two Gram-negative species (*Pseudomonas putida* and *Shewanella oneidensis*) were used separately to yield exudate solutions. Briefly, monocultures of each species were maintained as colonies on trypticase soy agar plates. A colony was transferred to 3 ml of autoclaved trypticase soy broth (TSB) with 0.5% yeast extract and incubated for 24 h at 32 °C. The 3 ml growth medium was then transferred to 1 L of the same growth medium and incubated for another 24 h on a shaking table at 32 °C, and harvested by centrifugation at 8500×*g* for 5 min. The resulting pellet was washed in 0.01 M $NaNO_3$ three times with centrifugation following each soak to remove residual growth medium. After the third wash, the biomass was decanted into a pre-weighed centrifuge tube, and the supernatant was separated and discarded following two 30 min centrifugation steps at 8500×*g* to yield a 'wet mass' of the biomass. This wet mass is the mass reported in this study, and for these species is approximately 5 times the dried mass. The washed and weighed biomass was soaked in 0.01 M $NaNO_3$ to produce the exudate solutions.

Exudate solutions were prepared after 4, 24, 48, and 72 h of soaking in order to test if the concentration or composition of the exudates produced were time-dependent. After the soaking step, the biomass suspensions were centrifuged at 8500×*g* for 5 min, and the supernatant was filtered through a 0.45 µM cellulose acetate membrane (Millipore) to isolate the aqueous exudate fraction for use in the experiments. Each bacterial species was cultured in three separate growths and each growth was prepared individually to produce experimental triplicates.

Potentiometric titrations

We conducted potentiometric titration experiments in order to determine the number of types of proton-active binding sites on the exudate molecules, and their site concentrations and acidity constant values. In potentiometric titrations, specific volumes of acid and/or base standards are added to a sample solution, and the resulting change in pH is measured after a brief equilibration time. These data yield model-independent measurements of the total concentration of proton-active sites present in the sample, and model-dependent values of the distinct acidity constant values and corresponding individual site concentrations (Fein et al. 2005). We conducted these experiments using the general protocol described by Yu et al. (2014). The titrations were performed using a Mettler Toledo T7 autotitrator. The automated buret assembly added aliquots of 1.001 M HCl or 1.011 M NaOH with a potentiometric stability of 0.01 mV/s required between titrant additions.

Each exudate solution was first acidified to pH 3.0. A forward or 'up-pH' titration was then conducted by basifying to pH 9.7, and the pH and volume of base added were recorded at each step. Similarly, a reverse or 'down-pH' titration was conducted for several of the exudate solutions by acidifying back to pH 3.0, again recording pH and volume of acid added at each step. Four NIST-standard pH buffer solutions (pH 2.00, 4.01, 7.00, and 10.00) were used to calibrate the instrument on each day of use. Prior to each titration, the exudate solution was purged with N_2 gas for at least 30 min to remove dissolved CO_2, and titrations were conducted in a closed polypropylene titration vessel into which N_2 gas was continuously supplied to the headspace to further exclude atmospheric CO_2. A Teflon-coated magnetic stir bar continuously stirred the solutions throughout the titration. Three biological replicates from different growth batches were measured for each cell soak time and for each bacterial species studied.

Potentiometric titration data modeling

The titration results were normalized to the mass of bacteria used to generate each exudate solution, and are presented as a biomass normalized net concentration of protons added to solution:

$$(Ca - Cb)/(g\ \text{bacteria/L}) \quad (1)$$

where Ca is the total concentration of acid added to the system and Cb is the total concentration of base added, both in moles per L. (g bacteria/L) represents the concentration of bacteria that was used to generate the exudate solution in question (g of bacteria, wet mass, per L solution during the

soak phase). Chemical equilibrium modeling of the data was conducted using FITEQL 2.0 (Westall 1982) with a discrete site model of the reactivity of the bacterial exudate functional groups, following the approach of Fein et al. (2005) and Seders and Fein (2011). Potentiometric titration experiments are essentially proton adsorption measurements, but they are conducted in systems in which it is impossible to track the total absolute concentration of H as one might do with a bulk metal adsorption experiment (Churchill et al. 1995; Fein et al. 2005). Therefore, instead of constraining the calculations using a mass balance on the absolute H concentration, modeling of potentiometric titration data uses a mass balance on the excess/deficit of protons associated with the titrated molecules relative to an arbitrarily defined zero proton condition. In this study, following the approach of potentiometric titration experiments involving bacterial suspensions (e.g., Fein et al. 2005), we define the zero proton condition as that at which the binding sites on the bacterial exudates are fully protonated. We model the proton buffering behavior of the exudate molecules as simple organic acid functional group sites, where the deficit of protons is represented as:

$$R - L_i H^0 \leftrightarrow R - L_i^- + H^+ \quad (2)$$

where L_i represents a proton-active functional group type, and R- represents the exudate molecule to which the functional groups are attached. The equilibrium constant for Reaction (2), termed the acidity constant, is expressed as:

$$K_{a(i)} = \frac{a_{R-L_i^-} \cdot a_{H^+}}{a_{R-L_i H^0}} \quad (3)$$

where a represents the activity of the subscripted species in solution. Equilibrium constants for the dissociation of water and sodium hydroxide were obtained from Smith and Martell (1989). Activity coefficients for ionic aqueous species were calculated using the Davies equation within FITEQL (Westall 1982), and activity coefficients of neutral species were assumed to be 1. The potentiometric titration data were used to determine how many types of sites are required to account for the observed buffering behavior of the exudate solutions, and to solve for the pKa(i) values, as well as for the concentrations, of each site type, i. The calculated site concentrations were normalized to the initial bacterial concentration (in g per L) used to generate each exudate solution. For comparison purposes, the total site concentration was calculated for each dataset and averaged for each experimental condition (that is, for each source bacterial species and time of cell suspension). Models with 1 to 4 discrete proton binding site types were tested for their fits to the model data. The goodness-of-fit of each model for each titration dataset was determined based upon the calculated variance parameter, V(Y), as calculated by the FITEQL program. A V(Y) value of 1 indicates a perfect fit, and values lower than 20 can be considered good fits to the data (Westall 1982).

Dissolved organic carbon analyses

We measured the concentration of dissolved organic carbon (DOC) present in each exudate sample studied here in order to determine if observed differences in buffering capacity were related to the total concentration of exudate molecules present in each sample. Samples for DOC analysis were prepared by diluting 2.5 mL of each individual exudate solution, harvested at every timepoint, with 12.5 mL of 0.01 M $NaNO_3$ and then acidified with 400 µL of 5% HNO_3. A range of standards from 0 to 800 ppm were prepared using a commercial 1000 ppm carbon standard stock (VWR), diluted and acidified to match the sample matrix. The standard curve and samples were analyzed on a Shimadzu TOC-L system. Technical replicates of the standard curve yielded an analytical uncertainty of ± 4% (1 standard deviation) for this method.

LIVE/DEAD staining and imaging

Samples of bacterial biomass from each species were collected at the same time as each exudate solution was sampled in order to determine the cell viability and thereby to constrain the origin of the exudate molecules as a function of time and between bacterial species. Although only qualitative relationships can be determined from these measurements, a higher proportion of dead cells suggests that cell lysis plays a relatively larger role in exudate production compared to samples with a lower proportion of dead cells. Two fluorophores were used to differentiate between living and dead cells: propidium iodide, which binds to DNA and fluoresces red but is unable to pass through an intact cell membrane and SYTO24, which also binds to nucleic acids but is membrane permeable and fluoresces green. When incubated with a mix of both dyes, cells with damaged membranes take up both green and red fluorophores, while living cells only take up green. The viability of the biomass is then determined by quantifying the relative proportions of red and green signals. In order to stain the biomass, a 50 µL aliquot of a biomass suspension was incubated with 1 µL of 1 mM propidium iodide and 1 µL of 5 mM SYTO24 in DMSO (Thermo Fisher) for 15 min. Wet mount slides were prepared from the stained samples and imaged on a Nikon A1 confocal laser scanning microscope (CLSM) using a Plan APO 100x oil immersion objective with excitation wavelengths of 488 and 561.5 nm, and emission detection between 500 and 550 nm (SYTO24/green) and 570 to 620 nm (propidium iodide/red). The resulting images were exported for analysis in ImageJ. Red and green channel images were analyzed separately for each sample. The mean pixel intensity of the cells as well as the percentage of the field containing cells was calculated for each image, then a total fluorescence signal for each image was calculated by multiplying the mean pixel intensity by the percent of the field containing cells.

LCMS analyses

In order to measure sulfhydryl site concentrations on the exudate molecules, we used a liquid chromatography mass spectrometry (LC-MS) approach in conjunction with a blocker molecule, monobromo(trimethylammonio)bimane bromide (qBBr) that binds strongly and specifically with sulfhydryl binding sites (Yu and Fein 2024). qBBr has been shown to be sulfhydryl-specific in its binding, does not bind with protons itself, and is inert to binding onto carboxyl or phosphoryl binding sites (Yu et al. 2014). This method yields a detection limit of approximately 1 µM of sulfhydryl sites in solution.

In this approach, a calibration curve is constructed from qBBr reacted with known concentrations of the sulfhydryl-bearing molecule N-acetyl-L-cysteine (ACYS), yielding a relationship between the measured decrease observed in the qBBr peak area (between the ACYS-free and the ACYS-bearing solutions) and the known sulfhydryl concentration in each standard. Then for each exudate solution, two LC-MS measurements are made on the following solutions: (1) an exudate-free solution with a known concentration of qBBr; and (2) a parallel solution with the same concentration of qBBr, but also with the addition of an exudate sample with unknown sulfhydryl concentration. In the solution containing both qBBr and the exudate molecules, qBBr binds specifically and irreversibly to sulfhydryl sites on the exudate molecules (if present) and hence is transformed from unbound to bound qBBr. Therefore, the decrease in the LC-MS peak area corresponding to unbound qBBr between these two samples can be directly related to the sulfhydryl concentration in the exudate sample.

Samples were prepared using a 2000 nM qBBr stock diluted with 0.01 M $NaNO_3$ (the same ionic strength buffer as was used in the potentiometric titration experiments). The samples were analyzed on a Bruker microTOF-Q II electrospray ionization time-of-flight quadrupole mass spectrometer set in positive mode coupled to a Dionex Ultimate 3000 UHPLC system fitted with a Waters ACQUITY UPLC HSS T3 column. We used a 5 µL injection volume and eluted over a span of 5 minutes at a flow rate of 0.4 mL/min to separate our samples with 97.5% ultrapure water and 0.1% formic acid/2.5% acetonitrile and 0.1% formic acid as the solvent. Resulting spectra were processed using Bruker Compass Data Analysis 4.2. The m/z peak used to calculate unbound qBBr was 328.07 ± 0.05.

Results and discussion

The bacterial exudate solutions exhibited a significant buffering capacity over the pH range examined in this study (approximately pH 3–10), suggesting the presence of multiple proton-active functional group site types with a range of *Ka* values. Comparison of forward and reverse titrations of the exudate solutions (a representative pair of which is depicted in Figure 1) demonstrates the reversibility of the protonation reactions on the timescale of these experiments. Although some hysterysis occurs, the high and low pH ends of the titrations overlap, and the total differences in the mass normalized (Ca-Cb) value from each titration from one end of the titration to the other are the same within experimental uncertainty. This result indicates that the protonation/deprotonation reactions are fully and rapidly reversible, and in general justifies the use of chemical equilibrium modeling to account for the observed buffering behavior. However, the up-pH titrations are smoother and most similar to the buffering behavior of other dissolved organic ligands (e.g., Seders and Fein 2011), and hence in our subsequent modeling we use the up-pH titrations only.

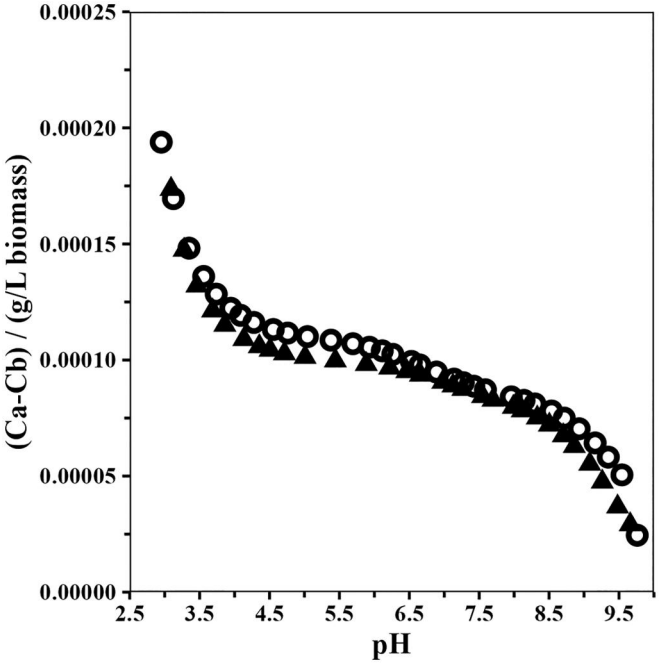

Figure 1. Representative titration of exudates from *P. putida* (20 g biomass/L, sampled at 48h). The down-pH titration is shown by open circles; the up-pH titration is shown by filled triangles.

We tested the fit of models with between 1 and 4 discrete proton-active binding site types to each of the potentiometric titration datasets, using FITEQL's V(Y) parameter to determine the best fitting model. For each titration in this study, a model with 3 site types (each with their own *Ka* and site concentration values) provides the best fit (Figure 2). For each titration dataset, the fit improves markedly with the addition of an additional proton-active binding site type, up to models with 4 binding site types, none of which converge, indicating an over-constraint of the system. Although we refer to these as distinct site types, they represent the number of *Ka* values and associated site concentrations that are needed to account for the observed buffering capacity of the exudate solutions over the pH range studied, and do not necessarily refer to chemically-distinct types of sites (carboxyl, phosphoryl, sulfhydryl, etc.). It is likely that each site 'type' defined here actually represents a range of chemical entities with similar protonation-deprotonation behaviors.

The averaged results of the chemical equilibrium modeling of the potentiometric titration data are compiled in Table 1 for the exudate solutions from the 4 bacterial species studied here, and for the 4 time periods of cell soaking for each species. It should be noted that different types of

models than the non-electrostatic model that we used (e.g., ones assuming Gaussian distributions of *Ka* values about an average) would yield different numbers of site types, *Ka* values, and individual site concentrations, but the calculated total site concentrations are a direct reflection of the titration data and are model independent.

The *Ka* values for each site derived from the modeled data do not exhibit significant variation between species or as a function of the soak time used to produce the exudates (Figure 3).

In contrast, individual site concentrations as well as total site concentrations increase as a function of soak time for all species studied (Figure 4). After 4 h of soak time, the 4 bacterial species exhibit similar site concentrations, but at all other soak times, the exudates from the Gram-positive species (*B. subtilis* and *B. licheniformis*) have significantly higher concentrations of each site type than the exudates from the Gram-negative species (*P. putida* and *S. oneidensis*). After 4 h, the *B. licheniformis* exudates exhibit the highest concentrations of each site type. At 24 h, the *B. subtilis* exudates site concentrations in general are intermediate between those of *B. licheniformis* and the two Gram-negative species, and after 24 h, the site concentrations in the exudates from the two Gram-positive species are not statistically different from each other, and the site concentrations in the exudates from the two Gram-negative species also are not statistically different from each other.

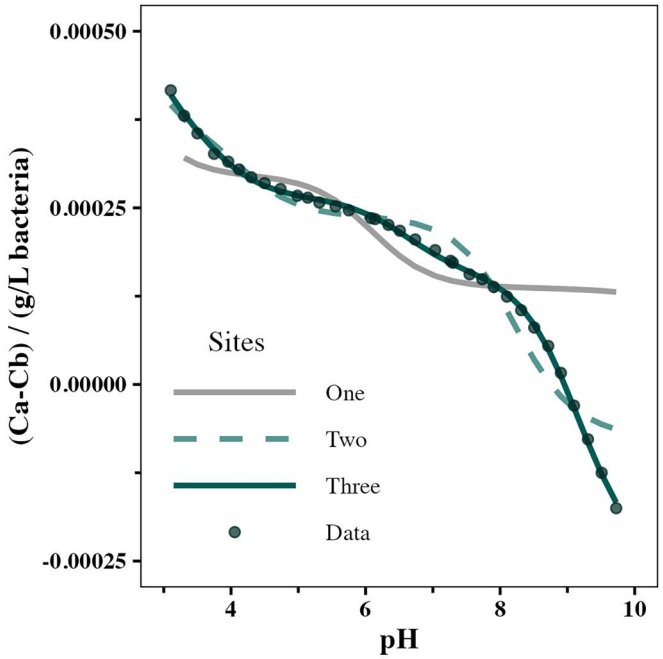

Figure 2. Representative model fits to potentiometric titration data (exudate solution from *B. subtilis* cells soaked in 0.01 M $NaNO_3$ for 48 h shown) modeled using 1-, 2-, and 3-site models.

The site concentration behavior as a function of species and soak time is mirrored in the DOC values for each exudate solution. Figure 5 illustrates that the DOC values of all of the exudate solutions after 4 h of soak time are similar, but for longer soak times, the exudate solutions from the Gram-positive species have significantly higher DOC values in almost all cases than the DOC values of the exudate solutions from the Gram-negative species.

The similarity between the time dependence of the DOC concentrations and the time dependence of the site concentrations suggests a strong relationship between the two parameters. Figure 6 demonstrates that total site concentrations exhibit a strong positive correlation to DOC concentrations in the exudate solutions as a whole. While Figure 4 indicates that significant differences are present in the characteristics of exudates produced at different soak times or by different species, Figure 6 demonstrates that a single relationship between DOC concentration and total site concentration can explain the variation in buffering capacity both as a function of soak time and between species. Our results indicate that there is no significant species-specific total protonation behavior and that in effect, the exudates produced by each species at all soak times exhibit the same total protonation behavior. The primary difference between any of the exudate solutions tested is the amount of dissolved

Table 1. Average values for calculated pKas and site concentrations using a 3-site model.

Parent Bacterial Species	Soak Time	pKa 1	[Site 1, μmol/g]	pKa 2	[Site 2, μmol/g]	pKa 3	[Site 3, μmol/g]	[Total sites, μmol/g]
B. subtilis								
	4 hours	4.17 ± 0.25	45.6 ± 14.1	6.7 ± 0.06	26.2 ± 7.3	9.08 ± 0.04	42.7 ± 18.3	114.4 ± 38.2
	24 hours	3.63 ± 0.37	83.9 ± 62.9	6.79 ± 0.12	61.3 ± 37.9	9.07 ± 0.08	186.8 ± 209.3	332.1 ± 309.1
	48 hours	3.64 ± 0.16	162.9 ± 34.4	6.58 ± 0.02	117 ± 39.6	9.15 ± 0.04	445.2 ± 232.6	725.2 ± 301.4
	72 hours	3.61 ± 0.44	115.6 ± 61.4	6.71 ± 0.10	142 ± 57.5	9.24 ± 0.08	497.8 ± 396.5	755.4 ± 337.6
P. putida								
	4 hours	4.17 ± 0.21	32.8 ± 9.7	6.14 ± 0.53	11.8 ± 3.6	9.20 ± 0.20	27.3 ± 5.3	72 ± 17.5
	24 hours	4.08 ± 0.51	55.2 ± 27.5	6.69 ± 0.12	21.5 ± 8.8	9.20 ± 0.13	41.2 ± 23.8	118 ± 52
	48 hours	3.85 ± 0.46	26.6 ± 8.8	6.82 ± 0.11	24.8 ± 12.3	9.27 ± 0.06	63.2 ± 11.1	114.7 ± 22.9
	72 hours	4.29 ± 0.44	16.5 ± 7	6.73 ± 0.07	40.8 ± 11.4	9.10 ± 0.14	88.9 ± 39	146.2 ± 23.6
S. oneidenensis								
	4 hours	3.77 ± 0.80	45.6 ± 22.2	6.23 ± 0.53	11.9 ± 4	9.15 ± 0.17	33 ± 18	90.6 ± 43.9
	24 hours	3.77 ± 0.25	25.7 ± 2.7	6.80 ± 0.09	19.1 ± 7.3	9.24 ± 0.03	52.1 ± 14.3	97 ± 23.8
	48 hours	3.35 ± 0.49	40.8 ± 19.5	6.81 ± 0.04	28.2 ± 9	9.17 ± 0.18	55.3 ± 37.7	124.5 ± 59
	72 hours	3.37 ± 0.14	38.8 ± 7.1	6.82 ± 0.14	52.4 ± 25	9.23 ± 0.04	153.3 ± 104.6	244.5 ± 122.4
B. licheniformis								
	4 hours	3.93 ± 0.09	72 ± 5.2	6.09 ± 0.05	37.5 ± 2.2	8.96 ± 0.09	69.9 ± 6.8	179.5 ± 6.3
	24 hours	3.66 ± 0.10	273.3 ± 131.2	6.18 ± 0.38	112 ± 7.7	8.91 ± 0.37	422 ± 275.6	807.4 ± 412.4
	48 hours	3.49 ± 0.06	272.2 ± 50.5	6.76 ± 0.06	85.7 ± 8.4	9.28 ± 0.05	545.7 ± 189.1	903.7 ± 145.5
	72 hours	3.53 ± 0.25	235.6 ± 146.8	6.82 ± 0.03	106 ± 4.7	9.30 ± 0.02	547.7 ± 277.8	889.4 ± 351.3

Values in the table are averages with 1σ standard deviation values from triplicate titrations for each condition studied. Site concentrations are reported in μmol/g of biomass used to produce the exudates.

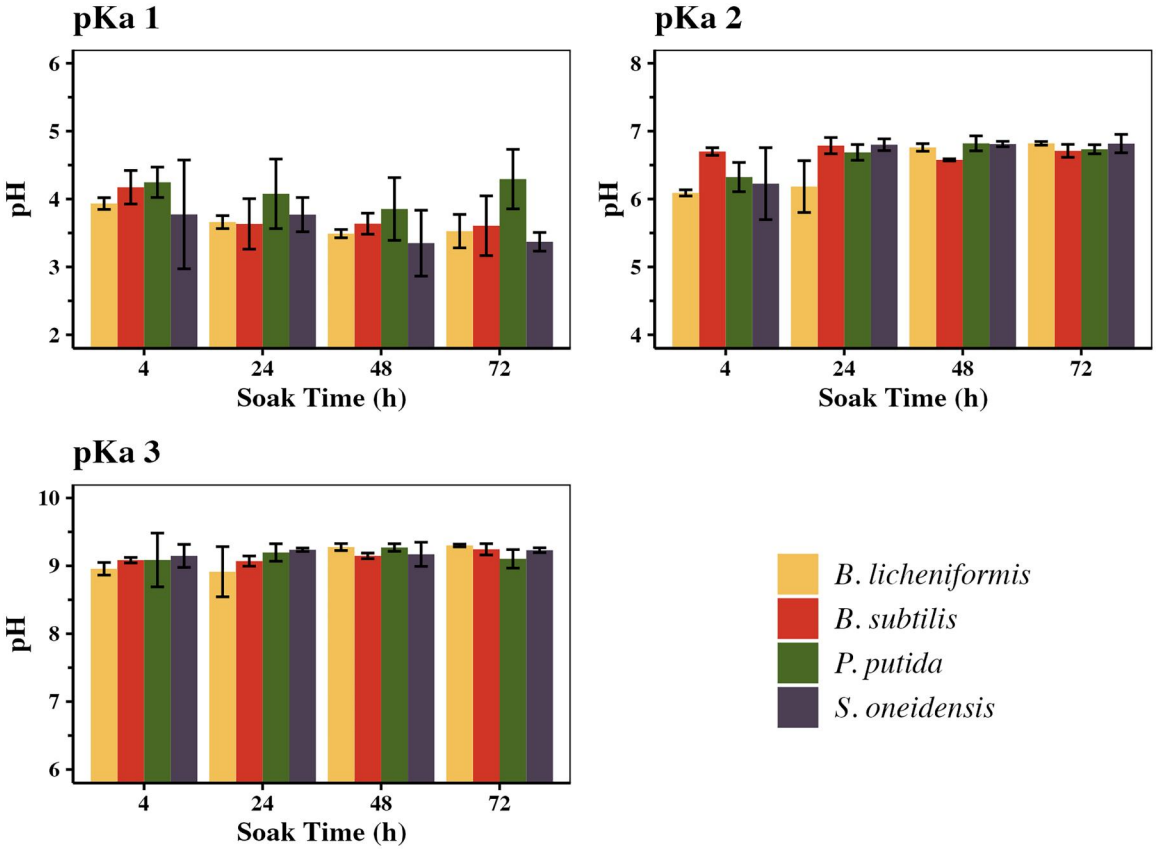

Figure 3. Average pKa values for each site, by species, as a function of soak time used to produce the exudate solutions. Error bars represent one standard deviation.

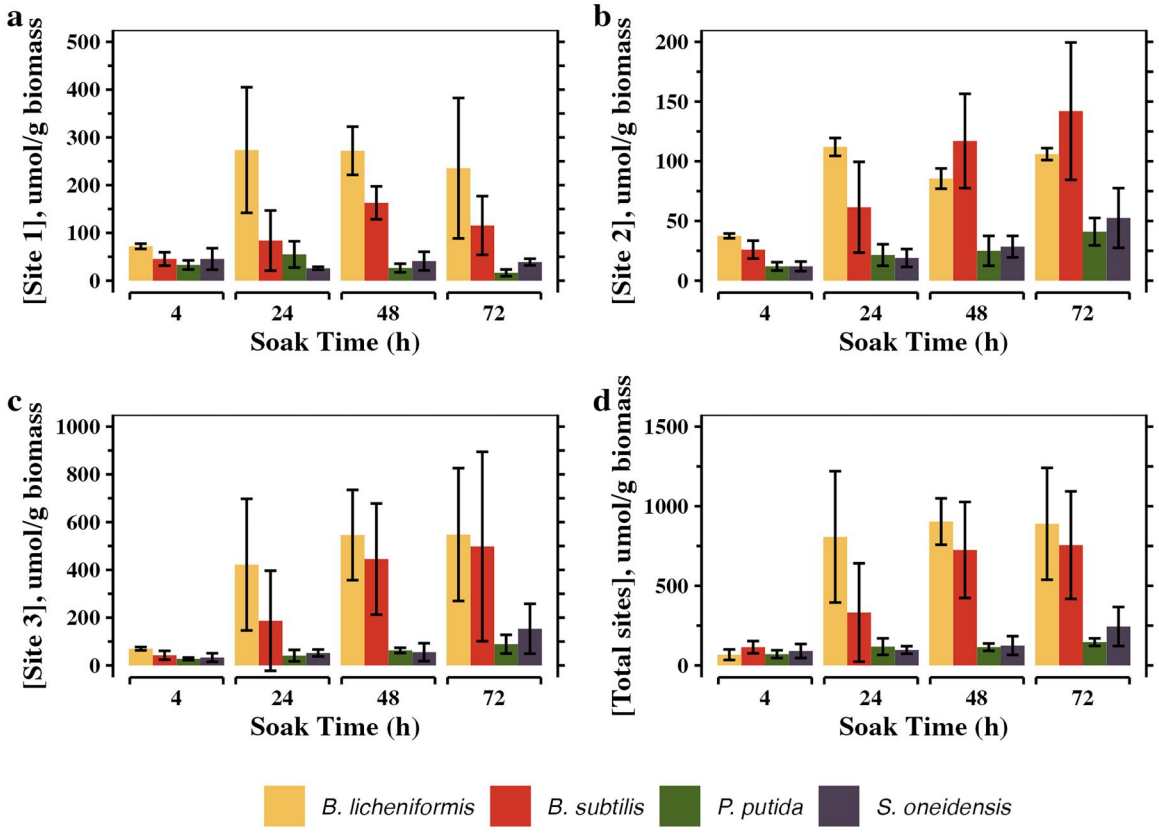

Figure 4. Average site concentrations (panels a-d: Site 1, site 2, site 3, total sites) as a function of soak time, by species. Error bars represent one standard deviation.

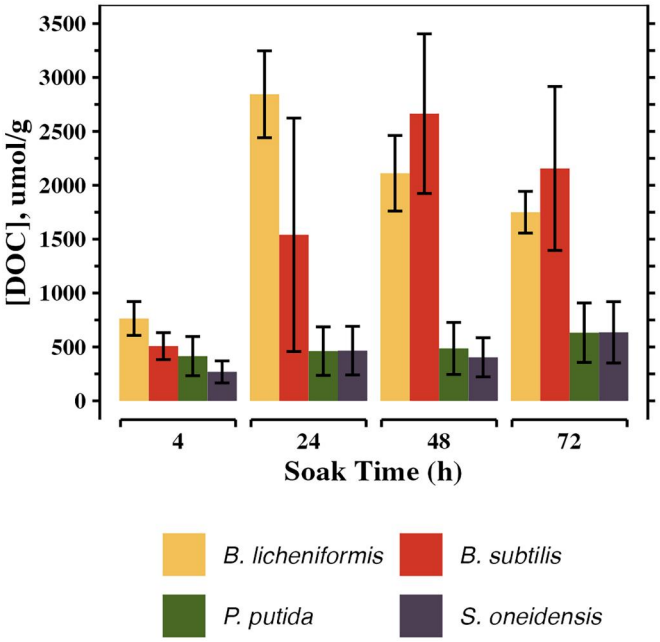

Figure 5. DOC concentrations as a function of soak time, by species. Error bars represent standard deviation.

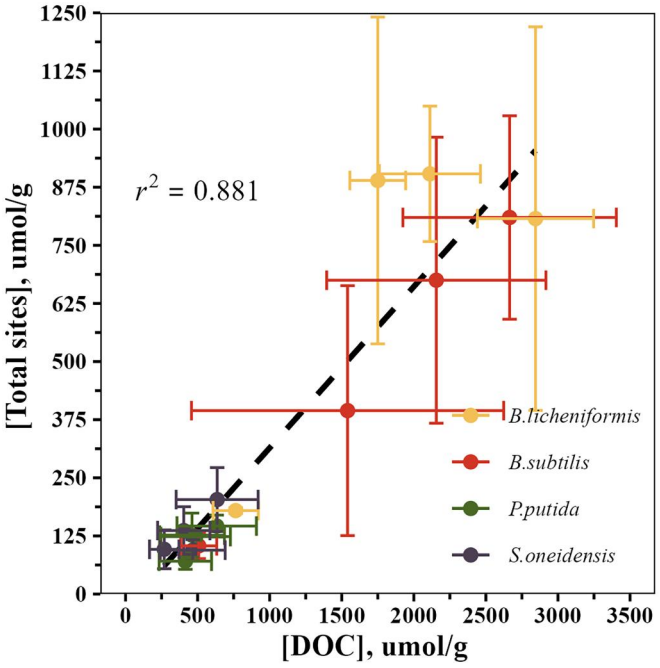

Figure 6. Total site concentration vs DOC concentration, by species. Error bars represent standard deviation.

organic material produced. While the exudates studied in Seders and Fein (2011) were harvested after a soak time of 2.5 h, the shortest soak time used in this study was 4 h. The average measured DOC concentration reported by Seders and Fein (2011) for the 2.5 h soak was approximately 3.1 ppm/g biomass while the 4 h exudates in this study had an average DOC concentration of 5.9 ppm/g biomass, nearly a 2-fold increase. This relationship is also present when comparing the concentration of total active sites between the two studies, with concentrations from the 2.5 h soak time from the Seders and Fein (2011) study and from the 4 h soak time from this study of 5.68×10^{-5} and 1.12×10^{-4} mol/g biomass, respectively, again just under a 2-fold increase. Longer soak times yield more exudate molecules, and the Gram-positive species studied yield more exudate molecules than the Gram-negative species studied, but the single relationship shown in Figure 6, and the consistency with the results from Seders and Fein (2011), strongly suggests that the total proton-binding behavior, and likely metal binding behavior as well, does not change markedly as a function of soak time or between bacterial species.

We normalized our calculated average individual site concentration values to DOC concentrations (Figure 7) in order to test if any species-specific differences exist. These DOC-normalized site concentrations exhibit markedly less variation as a function of soak time and between bacterial species than the non-normalized values shown in Figure 4. There are no systematic differences in any of the individual or total site concentrations between the exudates from different species at any of the soak times studied. And while the DOC-normalized concentrations of Sites 2 and 3 both increase slightly with soak time for exudates from some of the species, the overall effect is much less pronounced than for the non-normalized concentrations. Together, Figures 4–7 strongly suggest that the primary control on the concentration of individual and total proton-active sites in the exudate solutions is the extent of exudate production in each system, and that there are not large differences in the nature of the exudate molecules from different bacterial species or as a function of soak time. Suspensions of Gram-positive cells yield higher concentrations of the exudate than Gram-negative species, and the concentration of the exudate from all species increases with increasing soak time, but the proton binding properties of all of the exudates are similar. This result suggests that the total protonation behavior of exudates in natural or bacteria-bearing engineered systems could be described and quantified simply with a DOC measurement, and that a wide range of bacterial species yield similar exudate molecules that have similar total proton binding properties.

Bacterial exudates contain sulfhydryl binding sites that have high affinities for chalcophile elements. For example, Se(IV) reduction by bacterial exudates has been documented, and experiments with and without the sulfhydryl-specific blocking molecule qBBr have shown that the Se(IV) reduction by exudates is caused by Se(IV) binding onto exudate molecule sulfhydryl sites (Sullivan et al. 2022). The measurements in this study are the first to quantify the concentration of sulfhydryl sites on bacterial exudate molecules. In order to yield values which could be compared to other systems, the measured sulfhydryl concentrations were divided by the concentration of the cell suspension used to produce each exudate solution. Biomass-normalized sulfhydryl site concentrations were determined to be 0.3 ± 0.02, 0.1 ± 0.05, 0.12 ± 0.04, and 0.15 ± 0.06 µmol/g biomass for the exudates produced by *B. licheniformis*, *B. subtilis*, *P. putida*, and *S. oneidensis*, respectively. The total site concentrations of these exudate solutions under the same conditions varied from 115 to 903 µmol/g of biomass, and thus sulfhydryl sites

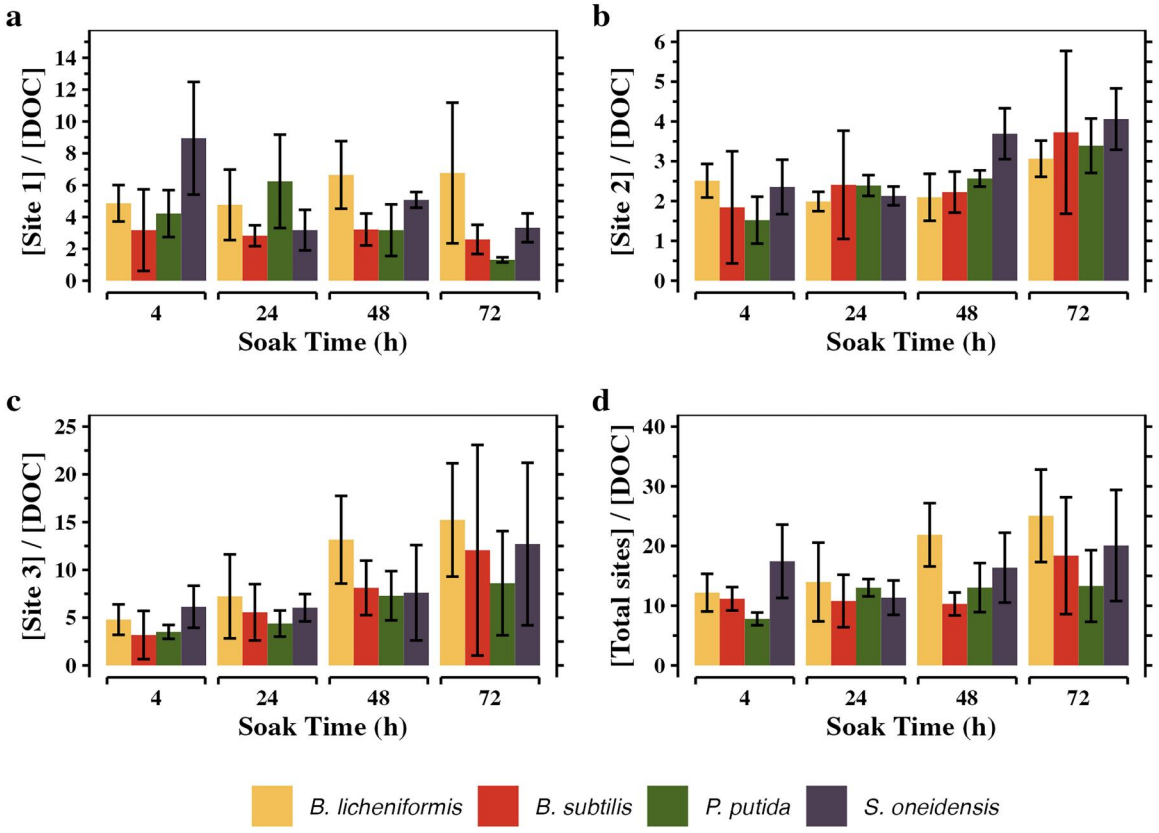

Figure 7. Average molar ratios of site concentrations (panels a-d: Site 1, site 2, site 3, total sites) as a function of soak time normalized by DOC concentration, by species. Error bars represent one standard deviation.

comprise less than 1% of the measured total concentration of proton-active binding sites on the exudate molecules. Sulfhydryl sites represent a smaller proportion of total proton-active binding sites on exudate molecules (less than 1%) than they do on cell surfaces (5–15%, depending on the species of bacteria; Yu et al. 2014). Despite their relatively low abundance, these sites can be the only means of exudate molecules to bind chalcophile elements and they play an outsized role in controlling processes such as Se(IV) binding and reduction by exudate molecules (Sullivan et al. 2022). The measured sulfhydryl site concentrations do not exhibit a simple relationship to the concentration of total proton-active sites on the exudate molecules (Figure 8). Exudates from *B. licheniformis* cells contain the highest concentration of sulfhydryl sites and also the highest total site concentration. However, the exudates from the other bacterial species studied each contain approximately $0.1-0.15\,\mu mol$ of sulfhydryl sites/g bacteria used to produce the exudates.

Our results suggest that the occurrence of sulfhydryl binding sites on exudate molecules is more species-dependent than are the DOC-normalized total site concentrations, individual site concentrations, or the calculated individual site pKa values, each of which are insensitive to species identity. Because sulfhydryl sites represent such a small proportion of total proton-active binding sites on the exudate molecules, their species-dependent concentration falls within the experimental uncertainty of the species-independent behavior that we measured for the individual and total site concentrations. Our exudate solutions, generated from approximately 20 g

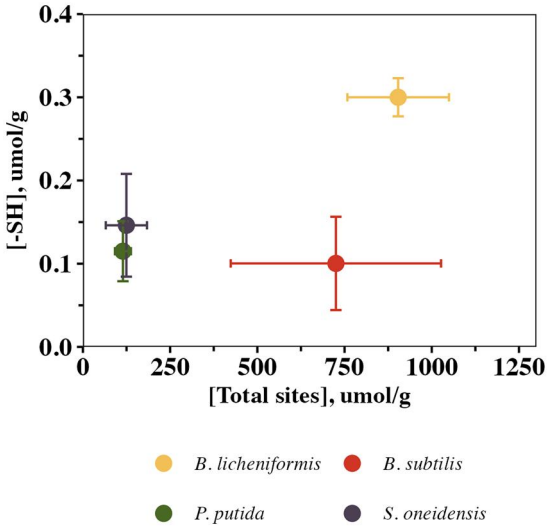

Figure 8. Sulfhydryl site concentrations versus total site concentrations of exudates produced by each species (20 g biomass/L, sampled at 48h). Error bars represent standard deviation.

biomass/L, contain 0.1–0.3 µmol of sulfhydryl sites/gram of biomass. In contrast, measured sulfhydryl site concentrations on bacterial cell walls range from approximately 20–33 µmol/g biomass (Joe-Wong et al. 2012; Yu et al. 2014). Our results indicate that sulfhydryl site concentrations on bacterial cell surfaces in a system containing a fixed mass of bacteria are approximately two orders of magnitude higher than those found on the exudate molecules produced from the same mass of bacteria. The higher concentration of sulfhydryl sites

on bacterial cell surfaces may facilitate the acquisition and uptake of trace chalcophile nutrients such as Se, Ni, and Zn from solution. However, it is possible that when bacteria grow under the stress of high concentrations of toxic chalcophile elements (e.g., Hg, Cd, Pb), then the cells could produce higher sulfhydryl site concentrations on their exudate molecules, as they do with solid phase EPS (Yu and Fein 2016) as a strategy for sequestering the toxins away from the cell. Even at the lower concentration of sulfhydryl sites on the exudate molecules that we have measured, exudates still can influence the environmental fate and mobility of chalcophile elements through sulfhydryl site binding, as exudates are soluble and mobile and thereby can influence the solubility and mobility of these elements as well. For example, bacterial exudates promote the reduction of Se(IV) to Se(0) by binding Se(IV) onto exudate sulfhydryl sites. Although the exudate-promoted reduction rate is slower than reduction by bacterial cells, the enhanced mobility of the dissolved exudate molecules suggests that their effect may be more widespread than that of cells within an immobile biofilm (Sullivan et al. 2022).

Exudate molecules can be either actively produced as a result of bacterial metabolic processes or passively released due to cell lysis after cell death and structural compromise of the cell wall. We used LIVE/DEAD staining to constrain the relative importance of these two processes (Figure 9). The Gram-positive species that we studied (Rows a & b) exhibited a higher proportion of dead cells at an earlier stage than the Gram-negative species (Rows c & d), which exhibited relatively little cell death during the course of the production of exudates. The Gram-positive cells also exhibited a dramatic decrease in the overall fluorescence by 48–72 h, which is consistent with extensive cell lysis occurring in these systems. In contrast, the overall fluorescence in the Gram-negative samples does not decrease markedly over the course of the 72 h experiment. Additionally, there is a significant negative correlation between total green fluorescence and DOC concentrations in the exudate solutions (Figure 10); i.e., the exudate samples from systems with the lowest number of live cells at 72 h contain the highest DOC concentrations. From this we infer that the large increase in DOC concentrations observed in the exudate solutions from the Gram-positive biomass is due primarily to cellular lysis, and not as a result of active production of exudate molecules from the cells.

Our study suggests that the differences in cell wall structure associated with Gram-negative and Gram-positive cell walls yield significant differences in the production of exudates through cell lysis. Under our experimental conditions, the inner and outer membranes of Gram-negative bacteria appear to maintain their structure, keep cells alive for longer, and yield lower exudate concentrations than does the simpler construction of the Gram-positive cell walls which lead to more cell death, cell lysis, and exudate production. The results of our LIVE/DEAD analysis suggest that the increase in overall proton-active sites in high-DOC samples is driven by passive production of exudates through cell lysis. In contrast, the lack of a relationship between the measured sulfhydryl site concentrations and the DOC of each sample indicates that sulfhydryl-bearing components of the exudate molecules are likely produced by active means and not as a passive byproduct of cell lysis. Our results suggest that DOC concentration measurements of bacteria-bearing systems represent an excellent proxy for total concentration of proton-active sites, but they cannot be used to estimate sulfhydryl site concentrations which appear to be independent of species and DOC values.

Conclusions

This study demonstrates that the primary control on the total proton binding properties of bacterial exudates is the amount of dissolved organic matter present, rather than inherent differences between the exudate molecules from different bacterial species or differences in exudate molecules as a function of soak time. In our experiments, Gram-positive bacteria released significantly more DOC than did Gram-negative bacteria, and we attribute this difference to the relative durability of the cell envelopes. The four bacterial species studied here each yielded exudate molecules with measurable concentrations of sulfhydryl sites, and this finding is consistent with qualitative observations of the involvement of exudate sulfhydryl sites in geochemical reactions (e.g., Se(IV) reduction; Sullivan et al. (2022). When normalized to DOC concentration, exudates from each species and from each soak time studied exhibited nearly identical total and individual site concentrations. In contrast, the measured sulfhydryl site concentrations for exudates produced from the four species studied here are independent of DOC concentrations of the exudate solutions. Sulfhydryl sites represent a small proportion of the total proton-active sites on the exudate molecules, and hence the lack of a relationship between sulfhydryl site concentrations and DOC is not inconsistent with the relationship between total site concentrations and DOC. Bacterial exudates are both actively produced by metabolic processes and passively released due to cell lysis. The observed relationships between total site concentrations and DOC concentrations, and between DOC concentrations and total green fluorescence in the LIVE/DEAD analysis, suggests that the vast majority of proton-active sites on the exudate molecules in our experiments originate from cell lysis. However, sulfhydryl site concentrations are independent of DOC concentrations and hence appear to be actively produced, as increases in cell lysis and the passive production of exudates do not lead to consistent increases in the concentration of sulfhydryl sites in the exudate samples. Sulfhydryl site concentrations in bacterial exudate solutions may vary in response to changes in cell growth conditions, but this remains undetermined.

Although bacterial cell surface binding sites and binding sites on solid-phase extracellular polymeric substances have received considerable attention, the environmental importance of proton and metal binding onto soluble bacterial exudate molecules is poorly characterized. We can use our results to estimate the importance of exudate binding sites in a soil setting. In these calculations, we assume a bacterial

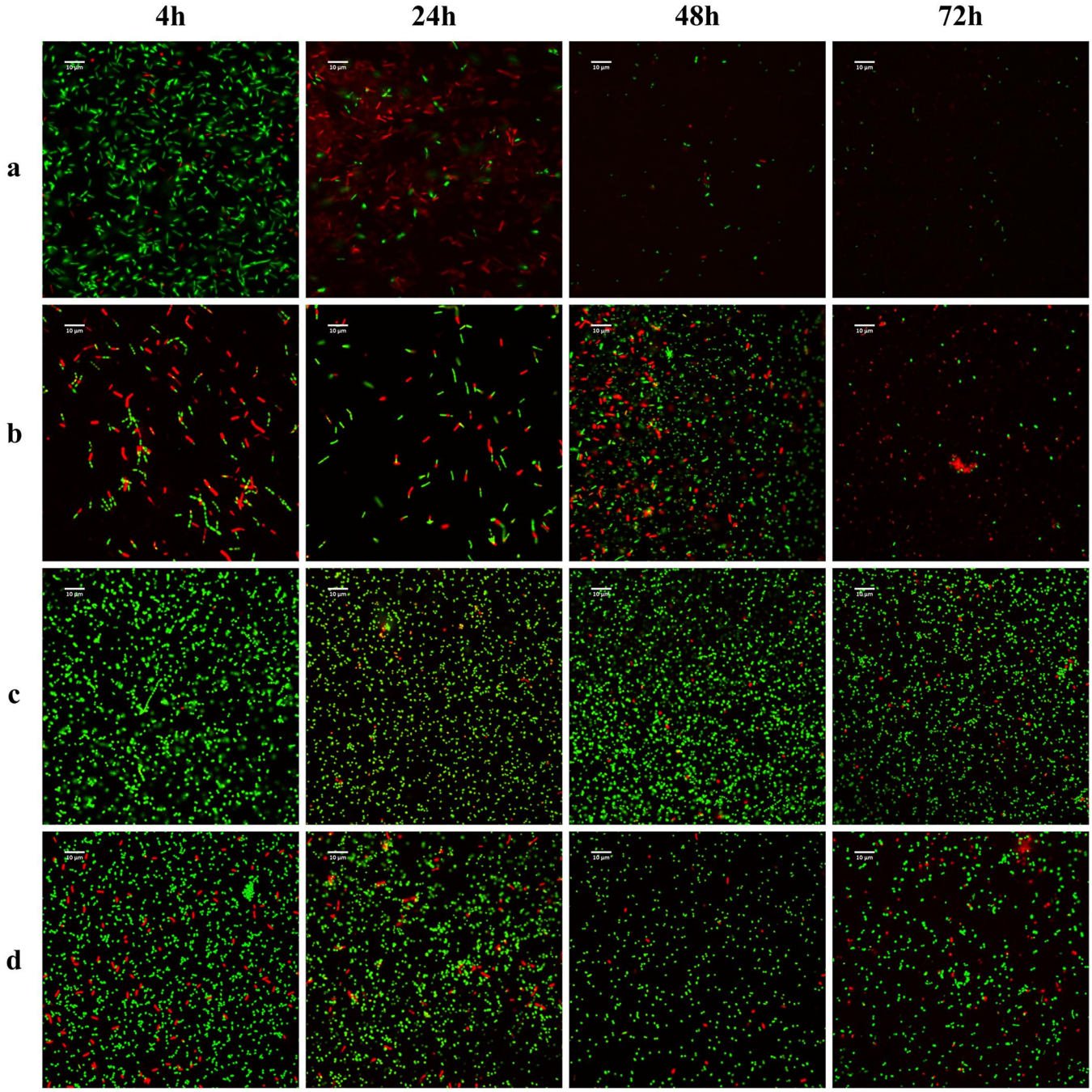

Figure 9. CLSM images of LIVE/DEAD stained cells after 4, 24, 48, and 72 h of soak time from *B. subtilis*, *B. licheniformis*, *P. putida*, and *S. oneidensis* (a–d) suspensions. Red fluorescence corresponds to dead cells; green corresponds to live cells. The white scale bar in the upper left of each image represents 10 μm.

cell number per gram of dry soil to be that given by Zhang et al. (2017) and we use a cell mass value from Neidhardt et al. (1990) to yield a reasonable estimate of the wet mass of biomass per gram of soil. This value can be used in conjunction with biomass normalized site concentrations for exudate molecules (from this study for both total sites and sulfhydryl sites, specifically) and for cell surfaces (taken from Borrok et al. (2005), for total sites, and from Joe-Wong et al. (2012), and from Yu et al. (2014), for sulfhydryl sites) to estimate the concentration of exudate-hosted and cell wall-hosted proton-active sites per gram of dry soil.

These calculations yield estimated exudate site concentrations of 4.7×10^{-7} moles of total sites and 1.6×10^{-10} moles of sulfhydryl sites per gram of dry soil, and estimated bacterial cell surface site concentrations of 3.1×10^{-7} moles of total sites and 2.3×10^{-8} moles of sulfhydryl sites per gram of dry soil. Our results suggest that sulfhydryl site concentrations are significantly lower on exudate molecules than on bacterial surfaces, but that the total concentration of proton-active sites is comparable. Additionally, although bacterial exudate molecules contain a lower concentration of sulfhydryl sites than are present on bacterial surfaces, because soluble exudate molecules are likely to be highly mobile in the environment, and because of their high affinity to bind chalcophile elements, it is likely that metal-exudates binding plays a significant role in the environmental transport

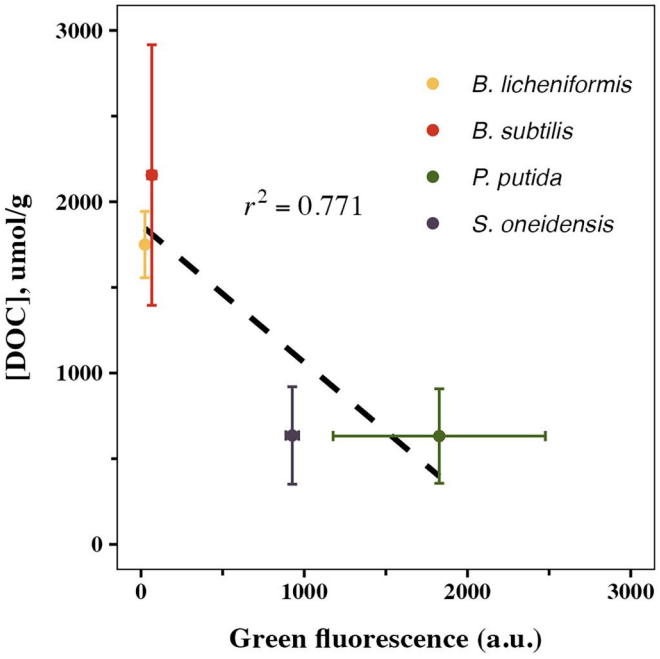

Figure 10. DOC vs green fluorescence signal (arbitrary units) for LIVE/DEAD stained biomass of each species (20 g biomass/L, sampled at 72 h). Error bars represent standard deviation.

and fate of these metals, and should be included when constructing quantitative models of metal cycling in geologic systems.

Disclosure statement

No potential conflict of interest was reported by the author(s).

Funding

Dissolved organic carbon analyses were performed in the Center for Environmental Science and Technology (CEST) at University of Notre Dame, and L.C.S. was partially supported by a CEST Predoctoral Research Fellowship. The research was funded in part by U.S. National Science Foundation Grant EAR-2149717.

References

Borrok D, Turner BF, Fein JB. 2005. A universal surface complexation framework for modeling proton binding onto bacterial surfaces in geologic settings. Am. J. Sci. 305(6-8):826–853.

Churchill SA, Walters JV, Churchill PF. 1995. Sorption of heavy metals by prepared bacterial cell surfaces. J Environ Eng 121(10):706–711.

Djemiel C, Dequiedt S, Karimi B, Cottin A, Horrigue W, Bailly A, Boutaleb A, Sadet-Bourgeteau S, Maron P-A, Chemidlin Prévost-Bouré N, et al. 2022. Potential of meta-omics to provide modern microbial indicators for monitoring soil quality and securing food production. Front Microbiol 13:889788.

Fein JB, Boily J-F, Yee N, Gorman-Lewis D, Turner BF. 2005. Potentiometric titrations of Bacillus subtilis cells to low pH and a comparison of modeling approaches. Geochim Cosmochim Acta 69(5):1123–1132.

Fomenko DE, Marino SM, Gladyshev VN. 2008. Functional diversity of cysteine residues in proteins and unique features of catalytic redox-active cysteines in thiol oxidoreductases. Mol Cells 26(3):228–235.

Giles NM, Watts AB, Giles GI, Fry FH, Littlechild JA, Jacob C. 2003. Metal and redox modulation of cysteine protein function. Chem Biol 10(8):677–693.

Joe-Wong C, Shoenfelt E, Hauser EJ, Crompton N, Myneni SCB. 2012. Estimation of reactive thiol concentrations in dissolved organic matter and bacterial cell membranes in aquatic systems. Environ Sci Technol 46(18):9854–9861.

Jones OAH, Sdepanian S, Lofts S, Svendsen C, Spurgeon DJ, Maguire ML, Griffin JL. 2014. Metabolomic analysis of soil communities can be used for pollution assessment. Environ Toxicol Chem 33(1):61–64.

Kawasaki N, Benner R. 2006. Bacterial release of dissolved organic matter during cell growth and decline: Molecular origin and composition. Limnol Oceanogr 51(5):2170–2180.

Keiblinger KM, Fuchs S, Zechmeister-Boltenstern S, Riedel K. 2016. Soil and leaf litter metaproteomics—a brief guideline from sampling to understanding. FEMS Microbiol Ecol 92(11):fiw180.

Kenney JPL, Song Z, Bunker BA, Fein JB. 2012. An experimental study of Au removal from solution by non-metabolizing bacterial cells and their exudates. Geochim Cosmochim Acta 87:51–60.

Neidhardt FC, Ingraham JL, Schaechter M. 1990. Physiology of the Bacterial Cell: A Molecular Approach. Sunderland, Mass: Sinauer Associates.

Ohnuki T, Yoshida T, Ozaki T, Kozai N, Sakamoto F, Nankawa T, Suzuki Y, Francis AJ. 2007. Chemical speciation and association of plutonium with bacteria, kaolinite clay, and their mixture. Environ Sci Technol 41(9):3134–3139.

Poole LB. 2015. The basics of thiols and cysteines in redox biology and chemistry. Free Radic Biol Med 80:148–157.

Rochfort S, Ezernieks V, Mele P, Kitching M. 2015. NMR metabolomics for soil analysis provide complementary, orthogonal data to MIR and traditional soil chemistry approaches – a land use study. Magn Reson Chem 53(9):719–725.

Seders LA, Fein JB. 2011. Proton binding of bacterial exudates determined through potentiometric titrations. Chem Geol 285(1–4):115–123.

Smith RM, Martell AE. 1989. Critical Stability Constants: Second Supplement. New York: Springer.

Sullivan LC, Boyanov MI, Wright JT, Warren MC, Kemner KM, Fein JB. 2022. Reduction of selenite by bacterial exudates. Geochim Cosmochim Acta 338:154–164.

Swenson TL, Jenkins S, Bowen BP, Northen TR. 2015. Untargeted soil metabolomics methods for analysis of extractable organic matter. Soil Biol Biochem 80:189–198.

Westall JC. 1982. FITEQL: A Computer Program for Determination of Chemical Equilibrium Constants from Experimental Data. Corvallis: Department of Chemistry, Oregon State University.

Yu Q, Boyanov MI, Liu J, Kemner KM, Fein JB. 2018. Adsorption of selenite onto Bacillus subtilis: the overlooked role of cell envelope sulfhydryl sites in the microbial conversion of Se(IV). Environ Sci Technol 52(18):10400–10407.

Yu Q, Fein JB. 2016. Sulfhydryl binding sites within bacterial extracellular polymeric substances. Environ Sci Technol 50(11):5498–5505.

Yu Q, Fein JB. 2024. Analysis of total thiol concentrations in environmental samples using ultra-high performance liquid chromatography-mass spectrometry (UHPLC-MS). Chem Geol. 644:121837.

Yu Q, Szymanowski J, Myneni SCB, Fein JB. 2014. Characterization of sulfhydryl sites within bacterial cell envelopes using selective site-blocking and potentiometric titrations. Chem Geol 373:50–58.

Zhang Z, Qu Y, Li S, Feng K, Wang S, Cai W, Liang Y, Li H, Xu M, Yin H, et al. 2017. Soil bacterial quantification approaches coupling with relative abundances reflecting the changes of taxa. Sci Rep 7(1):4837.